# Simple Approach for High-Contrast Optical Imaging and Characterization of Graphene-Based Sheets

Inhwa Jung,[†] Matthew Pelton,[‡] Richard Piner,[†] Dmitriy A. Dikin,[†] Sasha Stankovich,[†] Supinda Watcharotone,[†] Martina Hausner,[§] and Rodney S. Ruoff*,[†]

*Department of Mechanical Engineering, Northwestern University, Evanston, Illinois 60208, Center for Nanoscale Materials, Argonne National Laboratory, Argonne, Illinois 60439, and Department of Chemistry and Biology, Ryerson University, 350 Victoria Street, Toronto, Ontario M5B 2K3, Canada*

Received June 13, 2007; Revised Manuscript Received September 3, 2007

## ABSTRACT

A simple optical method is presented for identifying and measuring the effective optical properties of nanometer-thick, graphene-based materials, based on the use of substrates consisting of a thin dielectric layer on silicon. High contrast between the graphene-based materials and the substrate is obtained by choosing appropriate optical properties and thickness of the dielectric layer. The effective refractive index and optical absorption coefficient of graphene oxide, thermally reduced graphene oxide, and graphene are obtained by comparing the predicted and measured contrasts.

Identifying and characterizing a single nanometer-scale layer, or a small number of layers, of materials such as graphite, any of a number of clays, or metal dichalcogenides such as $WS_2$, is challenging yet critical for the study of such materials.[1,2] Scanning probe microscopy methods, such as atomic force microscopy (AFM), can both identify the presence of such thin sheets and determine their lateral and vertical dimensions.[3] Because these methods are time consuming at the resolution required to discriminate between single and bilayers of a material, the scan area must be restricted. Scanning electron microscopy can also, in principle, be used for identification of individual layers versus multilayer sheets, but this imaging typically induces the formation of a layer of contaminant in the exposed region.[4]

Optical methods, on the other hand, offer the potential for rapid, nondestructive characterization of large-area samples. Ellipsometry, for example, is widely used to determine the optical constants and thicknesses of thin films. Standard ellipsometers, though, require samples with lateral dimensions well over a millimeter. By contrast, imaging ellipsometry can have submicrometer resolution and may be useful for probing optical constants and thicknesses.[5,6] Investigations into this method are ongoing and will be reported elsewhere.

For the past two years, we have focused on simpler methods that allow the use of standard confocal microscopy for rapid identification and characterization of the optical response of thin sheets.[7,8]

In particular, we have investigated the use of substrates designed to interferometrically enhance the visibility of thin sheets. Interference techniques have been used for over half a century to allow for the imaging of low-contrast and transparent samples.[9,10] Over the past decade, microscopy of fluorescent monolayers has been enhanced by incorporating a thin dielectric layer between the material and a reflective substrate.[11] Fabry-Perot interference in the dielectric layer modulates the fluorescence intensity, allowing the determination of the thicknesses of surface layers with nanometer precision.[12] Recently, a similar method has been used for the identification of single graphene sheets.[1,2] Graphene monolayers and multilayers were deposited on substrates consisting of a silicon wafer with an intermediate, 300 nm thick silicon dioxide layer, and the monolayers were qualitatively identified by their weak contrast under white light illumination. The contrast between the graphene layers and the substrate has been modeled using a multilayer interference method.[13,14] It was thereby shown that contrast could be improved by using narrow band illumination, thereby allowing for the straightforward determination of the number of graphene layers.[15,16] Spectral resolution of the

* Corresponding author. Tel: (847) 467-6596. Fax: (847) 491-3915. E-mail: r-ruoff@northwestern.edu.
† Northwestern University.
‡ Argonne National Laboratory.
§ Ryerson University.

**Supporting Information Available:** Experimental procedure, calculation of the contrast, comparison of dielectric layers, and uncertainty of optimized optical properties. This material is available free of charge via the Internet at http://pubs.acs.org.

## References

(1) Novoselov, K. S.; Geim, A. K.; Morozov, S. V.; Jiang, D.; Zhang, Y.; Dubonos, S. V.; Grigorieva, I. V.; Firsov, A. A. *Science* **2004**, *306*, 666.

(2) Novoselov, K. S.; Jiang, D.; Schedin, F.; Booth, T. J.; Khotkevich, V. V.; Morozov, S. V.; Geim, A. K. *Proc. Natl. Acad. Sci. U.S.A.* **2005**, *102*, 10451.

(3) Piner, R. D.; Xu, T. T.; Fisher, F. T.; Qiao, Y.; Ruoff, R. S. *Langmuir* **2003**, *19*, 7995.

(4) Ding, W.; Dikin, D. A.; Chen, X.; Piner, R. D.; Ruoff, R. S.; Zussman, E.; Wang, X.; Li, X. *J. Appl. Phys.* **2005**, *98*, 014905.

(5) Zahn, Q.; Leger, J. R. *Appl. Opt.* **2002**, *41*, 4443.

(6) Beaglehole, D. *Rev. Sci. Instrum.* **1988**, *59*, 2557.

(7) Jung, I.; Piner, R.; Dikin D.; Stankovich, S.; Ruoff, R. S.; Hausner M. APS Meeting 2006, March 13−17, Baltimore, MD, (Abstract ID: BAPS.2006.MAR.D35.12, http://meetings.aps.org/link/BAPS.2006.MAR.D35.12).

(8) Jung, I.; Piner, R.; Dikin, D.; Stankovich, S.; Watcharotone, S.; Ruoff, R. S. APS Meeting 2007, March 5−9, Denver, CO, (Abstract ID: BAPS.2007.MAR.L28.13, http://meetings.aps.org/link/BAPS.2007.MAR.L28.13).

(9) Zernike, F. *Physica* **1942**, *9*, 686.

(10) Zernike, F. *Physica* **1942**, *9*, 974.

(11) Lambacher, A.; Fromherz, P. *Appl. Phys. A* **1996**, *63*, 207.

(12) Kiessling, V.; Tamm, L. K. *Biophys. J.* **2003**, *84*, 408.

(13) Abergel, D. S. L.; Russell, A.; Fal'ko, V. I. *Appl. Phys. Lett.* **2007**, *91*, 063125.

(14) Roddaro, S.; Pingue, P.; Piazza, V.; Pellegrini, V.; Beltram, F. *Nano Lett.* **2007**, *7*, 2707.

(15) Blake, P.; Novoselov, K. S.; Castro Neto, A. H.; Jiang, D.; Yang, R.; Booth, T. J.; Geim, A. K.; Hill, E. W. *Appl. Phys. Lett.* **2007**, *91*, 063124.

(16) Casiraghi, C.; Hartschuh, A.; Lidorikis, E.; Qian, H.; Harutyunyan, H.; Gokus, T.; Novoselov, K. S.; Ferrari, A. C. *Nano Lett.* **2007**, *7*, 2711.

(17) Ni, Z. H.; Wang, H. M.; Kasmin, J.; Fan, H. M.; Yu, T.; Wu, Y. H.; Feng, Y. P.; Shen, Z. X. *Nano Lett.* **2007**, *7*, 2758.

(18) Stankovich, S.; Piner, R. D.; Chen, X.; Wu, N.; Nguyen, S. T.; Ruoff, R. S. *J. Mat. Chem.* **2006**, *16*, 155.

(19) Hirata, M.; Gotou, T.; Horiuchi, S.; Fujiwara, M.; Ohba, M. *Carbon* **2004**, *42*, 2929.

(20) Stankovich, S.; Dikin, D. A.; Dommett, G. H. B.; Kohlhaas, K. M.; Zimney, E. J.; Stach, E. A.; Piner, R. D.; Nguyen, S. T.; Ruoff, R. S. *Nature* **2006**, *42*, 282.

(21) Ward, L. *The Optical Constants of Bulk Materials and Films*; Institute of Physics Publishing: Philadelphia, PA, 1994.

(22) Macleod, H. A. *Thin-film optical filters*; American Elsevier Publishing Company Inc.: New York, 1969.

(23) Möller, K. D. *Optics*; University Science Books: Mill Valley, CA, 1988.

(24) Michelson, A. *Studies in Optics*; University of Chicago Press: Chicago, IL, 1927.

(25) The thermal treatment changes the chemistry of the graphene oxide sheets, reducing the number of oxygen bonds. It thereby leads to a change in the chemical interaction among the graphene oxide layers and possibly also results in a reduction of their thicknesses. Partial removal of the intercalated water may also affect the measured thicknesses.

(26) Li, J. L.; Chun, J.; Wingreen, N. S.; Car, R.; Aksay, I. A.; Saville, D. A. *Phys. Rev. B* **2005**, *71*, 235412.

(27) Yoshizawa, K.; Yumura, T.; Yamabe, T.; Bandow, S. *J. Am. Chem. Soc.* **2000**, *122*, 11871.

(28) Vaupel, M.; Fuchs, K. Nanofilm Technologie GmbH, Goettingen, Germany. Private communication, 2006.

(29) Djurisic, A. B.; Li, E. H. *J. Appl. Phys.* **1999**, *85*, 7404.

NL0714177

# Deflection–voltage curve modelling in atomic force microscopy and its use in DC electrostatic manipulation of gold nanoparticles

## J Toset, I Casuso, J Samitier and G Gomila

Departament d'Electrònica, Universitat de Barcelona and Laboratori de
Nanobioenginyeria-CREBEC, Parc Científic de Barcelona, C/Josep Samitier 1-5,
08028 Barcelona, Spain

E-mail: jtoset@el.ub.es

## Abstract
A model of deflection–voltage curves in atomic force microscopy and its use
in DC electrostatic nanomanipulation experiments are presented. The
proposed model predicts the deflection of the atomic force microscope probe
as a function of the applied probe–substrate voltage, as well as the distance
and voltage at which the tip collapses irreversibly onto the substrate due to
electrostatic forces. The model is verified experimentally and its use in DC
electrostatic manipulation of 25 nm radius gold nanoparticles is
demonstrated.

(Some figures in this article are in colour only in the electronic version)

## 1. Introduction

In recent years there has been an increased interest in using electrical forces in atomic force microscopy (AFM) to manipulate nanoparticles [1–3]. In these experiments, a conductive atomic force microscope probe is used to localize the nanoparticle in any standard imaging mode, and is then used to pick up the nanoparticle by applying a voltage bias between the probe and the nanoparticle (figure 1). The existing demonstrations of nanoparticle electrical manipulation with AFM utilize AC voltages in order to make use of either dielectrophoretic forces [1, 2] or charging and discharging events [3]. AC electrical manipulation is primarily designed to be implemented with most kinds of nanoparticles in a liquid environment.

Until now no demonstration of the electrostatic manipulation of nanoparticles with DC voltages has been reported, in spite of analogous existing experiments with microparticles and microprobes [4–6]. DC electrostatic manipulation is primarily designed to be implemented with chargeable particles in a dry environment (e.g. air).

One of the possible explanations for this situation is that the voltage bias applied to attract the nanoparticle in a DC electrostatic AFM manipulation experiment simultaneously bends the AFM probe, very often resulting in the irreversible collapse of the probe onto the nanoparticle. In order to avoid this problem, detailed knowledge of the deflection–voltage properties of the AFM probe, including electrostatic collapse events, becomes necessary.

The present paper precisely addresses this issue by presenting a detailed model of the deflection–voltage curves in electrostatic atomic force microscopy applications, including electrostatic snap-in events. The present model goes beyond existing models for the electrostatic bending of AFM probes in electrostatic force microscopy (which do not include collapse events) [7, 8] as well as models for the collapse events of cantilevers and microstructures under electrostatic interaction [9, 10], which do not include the effect of the AFM tip. The proposed model describes the bending of the AFM probe under the action of an electrostatic force as well as the distance and applied voltage at which the tip collapses irreversibly onto the substrate.

The theoretical model presented is verified experimentally and its use in the realization of DC electrostatic nanomanipulation experiments is demonstrated via the manipulation of 25 nm radius gold nanoparticles.

images before and after the electrostatic nanomanipulation experiment.

## 5. Conclusions

We have presented an analytical model to determine the equilibrium tip–substrate distance in electrostatic AFM. For predetermined probe specifications, and initial separation distances between tip and substrate, we have demonstrated that the equilibrium distance follows a modified quadratic dependence on the applied voltage (due to the apex–substrate interaction) and that a critical applied bias exists for which the tip collapses to the substrate, from a given collapse distance. The collapse distance is shown to depend on the initial separation and to be independent of the spring constant (for a given tip geometry). Moreover, the voltage collapse has been shown to be dependent on the initial distance and the square root of the spring constant for a fixed initial distance. Theoretical results have been verified through experimentation.

Finally, we have shown how the derived model can be used to implement successful DC electrostatic nanoparticle manipulation experiments using AFM, and demonstrated the successful electrostatic manipulation of a 25 nm radius gold nanoparticle.

These results therefore offer a perspective on the considerations required for the manipulation of nanoparticles using AFM.

## Acknowledgments

## References

[1] Decossas S, Mazen F, Baron T, Brémond G and Souifi A 2003 *Nanotechnology* **14** 1272–8
[2] Lee H W, Kim S H, Kwak Y K, Lee E S and Han C S 2005 *Sensor Actuators* A **125** 41–9
[3] Kim J E and Han C S 2005 *Nanotechnology* **16** 2245–50
[4] Takahashi K, Kajihara H, Urago M and Saito S 2001 *J. Appl. Phys.* **90** 432–7
[5] Saito S, Himeno H and Takahashi K 2003 *J. Appl. Phys.* **93** 2219–24
[6] Saito S, Himeno H, Takahashi K and Urago M 2003 *Appl. Phys. Lett.* **83** 2076–8
[7] Gomez-Monivas S, Froufe-Perez LS and Caamaño A J 2001 *Appl. Phys. Lett.* **79** 4048–50
[8] Sacha G M and Saenz J J 2004 *Appl. Phys. Lett.* **85** 2610–2
[9] Willemsen O H, Snel M M E, Kuipers L, Figdor C G, Greve J and De Grooth B G 1999 *Biophys. J.* **76** 716–24
[10] Tas N, Sonnenberg T, Jansen H, Legtenberg R and Elwenspoek M 1996 *J. Micromech. Microeng.* **6** 385–97
[11] Gil A, Colchero J, Gomez-Herrero J and Baró M A 2003 *Nanotechnology* **14** 332–40
[12] Hudlet S, Saint Jean M, Guthmann C and Berger J 1998 *Eur. Phys. J.* B **2** 5–10
[13] Argento C and French R H 1996 *J. Appl. Phys.* **80** 6081–90
[14] Gomez-Navarro C, Gil A, Alvarez M, De Pablo P J, Moreno-Herrero F, Horcas I, Fernandez-Sanchez R, Colchero J, Gomez-Herrero J and Baró M A 2002 *Nanotechnology* **13** 314–7
[15] Li J L, Chun J, Wingreen N S, Car R, Aksay I A and Saville D A 2005 *Phys. Rev.* B **71** 235412

P H Y S I C A L  R E V I E W  L E T T E R S

# Orientational Order of Molecular Assemblies on Inorganic Crystals

D. A. Saville,[1] J. Chun,[1] J.-L. Li,[2] H. C. Schniepp,[1] R. Car,[2] and I. A. Aksay[1]

[1]*Department of Chemical Engineering, Princeton University, Princeton, New Jersey 08544, USA*
[2]*Department of Chemistry, Princeton University, Princeton, New Jersey 08544, USA*

Surfactant micelles form oriented arrays on crystalline substrates although registration is unexpected since the template unit cell is small compared to the size of a rodlike micelle. Interaction energy calculations based on molecular simulations reveal that orientational energy differences on a molecular scale are too small to explain matters. With atomic force microscopy, we show that orientational ordering is a dynamic, multimolecule process. Treating the cooperative processes as a balance between van der Waals torque on a large, rodlike micellar assembly and Brownian motion shows that orientation is favored.

PACS numbers: 82.70.Dd, 81.07.−b, 81.16.Dn, 82.70.Uv

Self-assembling surfactant micelles and proteins are of interest in the molecular level processing of materials with nanoscale structural design. Because of the fact that self-assembly involves multiple nucleation sites, the process often needs to be guided to control the structure at microscopic and larger length scales. Inorganic single crystals have been used as templates to guide the self-assembly of micelles and proteins with order that reflects the underlying crystal structure, although the reasons for the ordering are uncertain [1–5].

Orientational order on crystals has been studied in a variety of nonmicellar systems where it has been called epitaxy [6], quasiepitaxy [7], and van der Waals epitaxy [8]. However, Wanless and Ducker [9] demonstrated that the spacing of cylindrical micelles on a highly ordered pyrolytic graphite (HOPG) substrate is not an integer multiple of the graphite unit cell which excludes epitaxy as the governing mechanism. Forrest [10] reviewed the potential energy calculation basis of orientation for organic thin films where, to simplify matters, the adlayer energies of adjacent molecular units were lumped into simpler entities interacting with the substrate. Although this formalism yields the orientation from the minimum energy configuration, Forrest cautions that, in practice, ordering depends on the nonequilibrium conditions under which a film grows. Because potential energy minimization can be computationally intensive, geometrical lattice misfit algorithms have been developed [11,12]. Such methods are not successful with certain configurations since they do not account for the relative strengths of adsorbate-substrate interactions and are not applicable to long, linear molecules or rodlike assemblies. None of these methods is appropriate for surfactant adsorption for several reasons, e.g., the role of the water solvent is omitted and the fact that molecules access a large number of configurations at nonzero temperatures.

This Letter describes a study of the orientational order of a molecular assembly adsorbed on graphite in an aqueous environment. The micelle assembly is composed of surfactant molecules of cationic cetyltrimethyl ammonium chloride (CTAC) (with micelle diameters ∼10 times the crystal lattice size) spanning hundreds of lattice units of the template—HOPG. Using liquid-cell atomic force microscopy (AFM) in the double layer repulsion mode, it was previously shown that these micelles align with respect to the underlying HOPG crystal [1–4]. We confirmed the alignment with the underlying structure in our experiments. Then, using the same technique, we acquired the sequence of deflection images (Fig. 1) showing the dynamic competition between grains of two different orientations, $\beta$ and $\beta'$—the small difference in contrast between the two grains is most likely caused by an asymmetry of the AFM probe.

This dynamic behavior—not addressed in previous AFM studies [1–5]—prompts us to propose a mechanism where micelles continuously disintegrate and reform while retaining their orientational order along the $\beta$, $\beta'$, or $\beta''$ axes of the graphite crystal. This scenario is also in line with the continuous exchange of surfactants between micelles and bulk solution at small time scales [13]. To interpret this behavior, we model the system at two length scales, molecular and colloidal. At the molecular level, we investigate interaction energy differences between different orientations for a single molecule. These are too small to explain ordering so we move to a larger length scale to investigate orientational ordering in terms of an anisotropic van der Waals interaction. At the colloidal level, we demonstrate that a van der Waals torque on the assembly results from collective effects on the larger length scale. This formalism leads to orientation, bridges the length scales, and accounts for temperature effects.

To examine the behavior of individual surfactant molecules at the molecular scale, van der Waals interaction energies are computed for CTAC adsorbed on HOPG. First, for a given orientation, we use a standard density-

the micelle is perpendicular to the symmetry axis of graphite in accord with our experiment. In addition, the tendency for orientational ordering becomes significant as the assembly size increases, which can be understood as a collective effect due to the assembly of surfactant molecules. The formulation provides the relationship between the energy and orientational order using geometrical factors and physical properties.

Although our colloidal approach provides a satisfactory interpretation for the origin of orientational order, it still needs improvement. In its present form, (i) it cannot handle the dynamic nature of the micelle disintegration and reassembly, (ii) it treats the micelle as rigid rods instead of flexible entities, and (iii) the micellar rods are noninteracting. In spite of these deficiencies, the equilibrium orientational order by anisotropic van der Waals interaction and resulting torque capture the process at the colloidal level; the torque leads to a minimum energy configuration of molecular assembly. In addition, since the torque is dependent on the size of molecular assembly, small energy differences at the molecular scale are thereby assembled into a collective effect.

---

[1] S. Manne, J. P. Cleveland, H. E. Gaub, G. D. Stucky, and P. K. Hansma, Langmuir **10**, 4409 (1994).

[2] S. Manne and H. E. Gaub, Science **270**, 1480 (1995).

[3] I. A. Aksay, M. Trau, S. Manne, I. Honma, N. Yao, L. Zhou, P. Fenter, P. M. Eisenberger, and S. M. Gruner, Science **273**, 892 (1996).

[4] H. N. Patrick, G. G. Warr, S. Manne, and I. A. Aksay, Langmuir **13**, 4349 (1997).

[5] C. L. Brown, I. A. Aksay, D. A. Saville, and M. H. Hecht, J. Am. Chem. Soc. **124**, 6846 (2002).

[6] M. Hara, H. Sasabe, A. Yamada, and A. F. Garito, Jpn. J. Appl. Phys. **28**, L306 (1989).

[7] F. F. So and S. R. Forrest, Phys. Rev. Lett. **66**, 2649 (1991).

[8] A. Koma, Surf. Sci. **267**, 29 (1992).

[9] E. J. Wanless and W. A. Ducker, Langmuir **13**, 1463 (1997).

[10] S. R. Forrest, Chem. Rev. **97**, 1793 (1997).

[11] J. A. Last, D. E. Hooks, A. C. Hillier, and M. D. Ward, J. Phys. Chem. B **103**, 6723 (1999).

[12] M. D. Ward, Chem. Rev. **101**, 1697 (2001).

[13] D. F. Evans and H. Wennerström, *The Colloidal Domain* (VCH Publishers, New York, 1994).

[14] K. A. Sharp, A. Nicholls, R. F. Fine, and B. Honig, Science **252**, 106 (1991).

[15] The potential parameters are taken from the CHARMM program. See the details at http://www.charmm.org.

[16] V. A. Parsegian and G. H. Weiss, J. Adhesion **3**, 259 (1972).

[17] J. Chun, J.-L. Li, R. Car, I. A. Aksay, and D. A. Saville (unpublished).

[18] J.-L. Li, J. Chun, N. S. Wingreen, R. Car, I. A. Aksay, and D. A. Saville, Phys. Rev. B **71**, 235412 (2005).

[19] M. Doi and S. F. Edwards, *The Theory of Polymer Dynamics* (Clarendon Press, Oxford, 1986).

[20] W. B. Russel, D. A. Saville, and W. R. Schowalter, *Colloidal Dispersions* (Cambridge University Press, New York, 1989).

# Anisotropic Adsorption of Molecular Assemblies on Crystalline Surfaces

**Jaehun Chun,[†] Je-Luen Li,[‡] Roberto Car,[‡] Ilhan A. Aksay,[†] and Dudley A. Saville\*,[†]**

*Departments of Chemical Engineering and Chemistry, Princeton University, Princeton, New Jersey 08544-5263*

*Received: April 26, 2006; In Final Form: June 20, 2006*

Orientational order of surfactant micelles and proteins on crystalline templates has been observed but, given that the template unit cell is significantly smaller than the characteristic size of the adsorbate, this order cannot be attributed to lattice epitaxy. We interpret the template-directed orientation of rodlike molecular assemblies as arising from anisotropic van der Waals interactions between the assembly and crystalline surfaces where the anisotropic van der Waals interaction is calculated using the Lifshitz methodology. Provided the assembly is sufficiently large, substrate anisotropy provides a torque that overcomes rotational Brownian motion near the surface. The probability of a particular orientation is computed by solving a Smoluchowski equation that describes the balance between van der Waals and Brownian torques. Torque aligns both micelles and protein fibrils; the interaction energy is minimized when the assembly lies perpendicular to a symmetry axis of a crystalline substrate. Theoretical predictions agree with experiments for both hemi-cylindrical micelles and protein fibrils adsorbed on graphite.

## Introduction

Surfactants in aqueous solution form micelles due, in part, to the limited solubility of their hydrocarbon tails. Spherical, cylindrical, bilayer, and bicontinuous structures occur, depending on the characteristics of the molecules and their concentrations.[1] Atomic force microscope (AFM) studies show that, when these micelles adsorb on crystalline templates, they display an orientational order dictated by the crystal structure of the template.[2−7] Similar observations are made with proteins on highly ordered pyrolytic graphite (HOPG)[8,9] although the same proteins in solution display a "wavy" fibrillar structure.[10] The fact that adsorption produces well-defined configurations suggests that patterned structures can be organized at the nanometer length scale. Molecular assemblies are especially appealing as templates for building composite structures because the length scale is small, typically a few nanometers, and controlled by molecular architecture.

Orientational relationships appear insensitive to the composition of the adsorbate. For example, Aksay et al.[4] showed that cationic, hemi-cylindrical micelles of cetyltrimethylammonium chloride (CTAC) adsorb on HOPG in patterns with (three) preferred directions (Figure 1). While the micelles align perpendicular to the symmetry axes of graphite, individual surfactant molecules on the surface are oriented parallel to the axes. Identical orientational relations are observed when de novo synthetic proteins adsorb onto HOPG (Figure 2).[8,9] Not surprisingly, the directionality is absent on amorphous carbon (Figure 2B).[9]

Anisotropic adsorption of molecular assemblies has not been limited to micellar and protein systems. Organic thin films grown by vapor deposition of planar molecules commonly display orientational order on crystalline templates.[11−15] In addition, simple alkane molecules such as $C_{19}H_{40}$ and $C_{50}H_{102}$ show the alignment and domain formation on crystallite

\* Corresponding author. E-mail: dsaville@princeton.edu. Telephone: 609-258-4585. Fax: 609-258-6835.
† Department of Chemical Engineering.
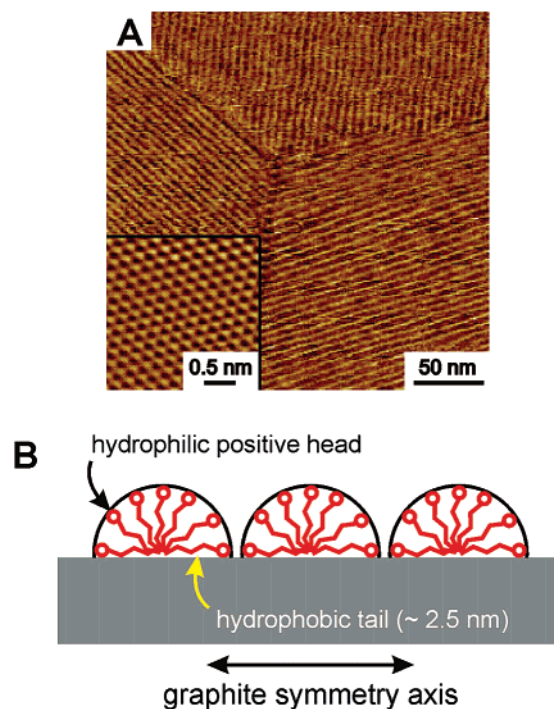‡ Department of Chemistry.

**Figure 1.** AFM image of hemi-cylindrical micellar assemblies of (A) cetyltrimethylammonium chloride (CTAC)[4] on HOPG. The underlying carbon lattice structure is shown in the inset in (A). The schematic side view (B) depicts hemi-cylindrical assemblies of CTAC. In the organized domains, the hemi-cylindrical rodlike micelles are aligned perpendicular to the symmetry axes.

templates.[16] Epitaxy,[17] quasi-epitaxy,[12] and van der Waals epitaxy[18] have been used to describe such ordered structures. Forrest[13] reviewed the potential energy (PE) calculation basis of orientational order for organic thin films where the adlayer energies of adjacent molecular units were lumped into simpler entities interacting with the substrate. However, simple addition of the PEs from isolated individual molecules on the crystalline surface is inadequate when dealing with crystal−water inter-

**TABLE B.1: Comparison between the Current Methodology and Extant Results for Several Systems in Terms of $A_{\mathrm{H}}^{\mathrm{iso}}$**

|  | current methodology[a] | experimental results | other theoretical calculations |
|---|---|---|---|
| graphite−water−graphite | 24 | 12.1−24[37,38] | 28[39] |
| graphite−air−graphite | 53 | 51−143[40] | 61[39] |
| hydrocarbon−water−hydrocarbon | 1.0 | ∼1.2[1] | − |

[a] The frequency mode summation is carried up to the ultraviolet region ($\sim 10^{17}$ (rad/s)) at 300 K. For graphite, $\beta$ was obtained at the zero wave vector limit.

principles method.[35] We adopted the tight-binding model approach in the current study. The energy levels $E_{n,\mathbf{k}}$ and other tight-binding parameters can be taken from the first-principles calculation. For energies below 15 eV, Lin et al.[34] showed the anisotropic dielectric response function of graphite for several wave vectors. In general, the imaginary dielectric response functions, $\alpha(i\xi_n, q_x)$ and $\beta(i\xi_n, q_y)$, are monotonically decreasing functions in the imaginary frequency $i\xi_n$. Their magnitudes also become smaller as **q** grows larger, so we model the wave vector dependence of $\gamma(i\xi_n, \mathbf{q})$ similar to the trend in $\alpha$ and $\beta$.

As a check of the calculated dielectric response functions, we used eq A.20 to evaluate Hamaker constants for several systems. Further discussion of the dielectric function of graphite can be found in Li et al.[36] Results are shown in Table B.1; our calculations are in accord with the experimental and theoretical results.[1,37−40]

The polar groups of the protein or surfactant molecule, which originate an intrinsic permanent dipole moment, merit a further comment here. We can set $f = 1.0$ and $\omega = 1.5 \times 10^{16}$(rad/s) for a typical nonpolar hydrocarbon in eq B.2. However, in the examples of the de novo designed protein,[8] one side of the $\beta$-sheet is made up of polar and charged residues. In the presence of charged residues, there will be counterions to neutralize the protein. As a result, the protein has a permanent dipole moment, and interactions of Debye-type (dipole−induced dipole) should be considered as a driving force in the orientational ordering of the self-assembly structure. In such cases, the mobile counterions near charged amino acids will give rise to a random and fluctuating dipole moment. The polarizability, and hence the magnitude of the dielectric response function, would be larger than the values we employed here. For a proper choice of $f$ and $\omega$ in eq B.2, the treatment in sections A and B can be carried over to a more general case where polar molecules are involved. In view of a larger dielectric constant, a larger anisotropy in the van der Waals interaction is expected.

### References and Notes

(1) Israelachvili, J. *Intermolecular and Surface Forces*; Academic Press: Boston, 1992.

(2) Manne, S.; Cleveland, J. P.; Gaub, H. E.; Stucky, G. D.; Hansma, P. K. *Langmuir* **1994**, *10*, 4409.

(3) Manne, S.; Gaub, H. E. *Science* **1995**, *270*, 1480.

(4) Aksay, I. A.; Trau, M.; Manne, S.; Honma, I.; Yao, N.; Zhou, L.; Fenter, P.; Eisenberger, P. M.; Grunner, S. M. *Science* **1996**, *273*, 892.

(5) Wanless, E. J.; Ducker, W. A. *J. Phys. Chem.* **1996**, *100*, 3207.

(6) Patrick, H. N.; Warr, G. G.; Manne, S.; Aksay, I. A. *Langmuir* **1997**, *13*, 4349.

(7) Saville, D. A.; Chun, J.; Li, J.-L.; Schniepp, H. C.; Car, R.; Aksay, I. A. *Phys. Rev. Lett.* **2006**, *96*, 18301.

(8) Brown, C. L.; Aksay, I. A.; Saville, D. A.; Hecht, M. H. *J. Am. Chem. Soc.* **2002**, *124*, 6846.

(9) Brown, C. L. Bachelor of Arts Thesis; Princeton University, Princeton, New Jersey, 2001.

(10) West, M. W.; Wang, W.; Patterson, J.; Mancias, J. D.; Beasley, J. R.; Hecht, M. H. *Proc. Natl. Acad. Sci. U.S.A.* **1999**, *96*, 11211.

(11) Novaco, A. D.; McTague, J. P. *Phys. Rev. Lett.* **1977**, *38*, 1286.

(12) So, F. F.; Forrest, S. R. *Phys. Rev. Lett.* **1991**, *66*, 2649.

(13) Forrest, S. R. *Chem. Rev.* **1997**, *97*, 1793.

(14) Last, J. A.; Hooks, D. E.; Hillier, A. C.; Ward, M. D. *J. Phys. Chem. B* **1999**, *103*, 6723.

(15) Ward, M. D. *Chem. Rev.* **2001**, *101*, 1697.

(16) Rabe, J. P.; Buchholz, S. *Science* **1991**, *253*, 424.

(17) Hara, M.; Sasabe, H.; Yamada, A.; Garito, A. F. *Jpn. J. Appl. Phys.* **1989**, *28*, L309.

(18) Koma, A. *Surf. Sci.* **1992**, *267*, 29.

(19) Wanless, E. J.; Ducker, W. A. *Langmuir* **1997**, *13*, 1463.

(20) Evans, D. F.; Wennerström, H. *The Colloidal Domain*; VCH Publishers: New York, 1994.

(21) Interactions due to permanent dipoles may also play a role in anisotropic adsorption. The methodology set out here can be generalized to include such contributions, cf., Appendix B.

(22) Parsegian, V. A.; Weiss, G. H. *J. Adhesion* **1972**, *3*, 259.

(23) Doi, M.; Edwards, S. F. *The Theory of Polymer Dynamics*; Clarendon Press: Oxford, 1986.

(24) Press, W. H.; Teukolsky, S. A.; Vetterling, W. T.; Flannery, B. P. *Numerical Recipes in FORTRAN*; Cambridge University Press: Cambridge, 1992.

(25) Hunter, R. J. *Foundations of Colloid Science*; Clarendon Press: Oxford, 1986; Vol. I.

(26) Cates, M. E. *Macromolecules* **1987**, *20*, 2289.

(27) Cates, M. E.; Candau, S. J. *J. Phys.: Condens. Matter* **1990**, *2*, 6869.

(28) Landau, L. D.; Lifshitz, E. M. *Theory of Elasticity*; Pergamon Press: New York, 1986.

(29) Parsegian, V. A. *J. Chem. Phys.* **1972**, *56*, 4393.

(30) Russel, W. B.; Saville, D. A.; Schowalter, W. R. *Colloidal Dispersions*; Cambridge University Press: New York, 1989.

(31) Honig, B.; Nicholls, A. *Science* **1995**, *268*, 1144.

(32) Mahanty, J.; Ninham, B. W. *Dispersion Forces*; Academic Press: New York, 1976.

(33) Djurisic, A. B.; Li, E. H. *J. Appl. Phys.* **1999**, *85*, 7404.

(34) Lin, M. F.; Huang, C. S.; Chou, D. S. *Phys. Rev. B* **1997**, *55*, 13961.

(35) Ahuja, R.; Auluck, S.; Wills, J. M.; Alouani, M.; Johansson, M.; Eriksson, O. *Phys. Rev. B* **1997**, *55*, 4999.

(36) Li, J.-L.; Chun, J.; Wingreen, N. S.; Car, R.; Aksay, I. A.; Saville, D. A. *Phys. Rev. B* **2005**, *71*, 235412.

(37) Hartley, P. A.; Parfitt, G. D. *Langmuir* **1985**, *1*, 651.

(38) Hartley, P. A.; Parfitt, G. D.; Pollack, L. B. *Powder Technol.* **1985**, *42*, 35.

(39) Dagastine, R. R.; Prieve, D. C.; White, L. R. *J. Colloid Interface Sci.* **2002**, *249*, 78.

(40) Parfitt, G. D.; Picton, N. H. *Trans. Faraday Soc.* **1968**, *64*, 1955.